

Comparison of design rules regarding the wing-body junction flow of a subsonic aircraft

University of Technology Kosice, Faculty of Aeronautics, Dep. of Aerodynamics

Sascha Siegel, student at University of Technology Dresden

30. June 2011

In this work a summary about existing design rules of the wing-body junction for subsonic airspeeds will be done. Different approaches and upcoming suggestions for reducing drag and improving flight performance that can be found in the literature are presented. Main focus is layed upon wing root fillets, wing-body positioning and fuselage design. Some alternative investigations concerning obstacles and suction holes in front of the wing are mentioned.

1 Introduction

In the ongoing process of aircraft development it is necessary to take a close look on every design detail. With the aim to reduce aerodynamic drag, improve flying abilities and endurance, the junction between wing and body of an aircraft is of great interest. Junction is a term for the connection of bodies with different shapes, in this special case the wing airfoil and the free-form shaped body of the aircraft. This junction induces interactions of the aerodynamic flow which cannot be explained with simple superposition of the two single body flows. Especially the combined boundary layers cause a flow phenomena difficult to describe and simulate, see section 2. In order to achieve improvements, there are several ways to manipulate the flow around the junction:

- Optimize the relative wing-body position (section 3.1)
- Adapt the junction shape with fillets and fairings (section 3.2 and 3.3)
- Manipulate the flow with active installations (section 3.4)

Extensive experimental research was done in the past, to mention the broad investigations by Eastman, Jacobs and Ward [3] and fillet-specific investigation by Muttray ([1] and [2]). The drag characteristics of wing-body junctions were summarized by Hoerner, ([4], chapter 8) and Schlichting/Truckenbrodt ([5], chapter 10.215). Later research with improved measurement systems and numerical simulation made it possible to focus on the flow phenomena itself. Remarkable investigations were made by Fleming et al. [6], extensive measurements can be obtained from Ölcmen [7] and a detailed summary is given by Simpson [8].

2 Flow around a junction

For understanding the flow phenomena, Simpson [8] gives an excellent description of the flow around an symmetric airfoil attached to a wall. A NACA 0020 tail cylinder with elliptic nose ($a/b = 2/3$) and thickness to chord ratio of $t/c = 0.24$ was used in his experiments (see figure 1.1). A plane top view of the flow around the junction is given in figure 1.2.

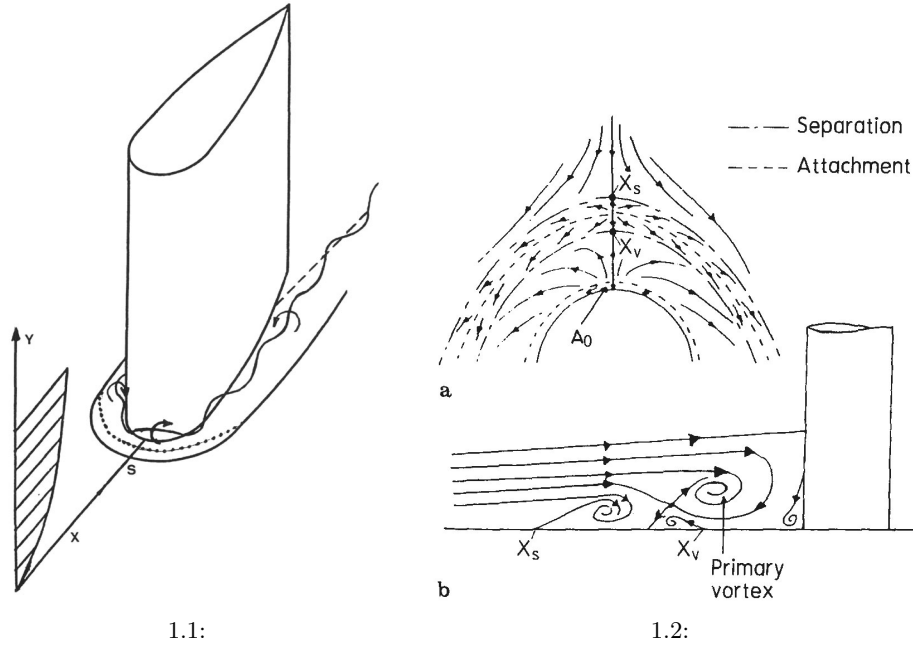


Figure 1: 1.1 NACA 0020 Tail Cylinder with elliptic nose (Rood Wing) in subsonic airflow. Separation line (solid) goes through the mean flow saddle point S. Dotted line shows low mean shear line for turbulent case. Horseshoe Vortex system originates at the leading edge corner. Reprint from [8]

1.2 Sketch of oil flow visualization of junction flow a) around a cylinder nose b) in the leading edge corner Reprinting from [6]

The airflow and wake phenomena depends on several influences:

- geometric influences
 - Height to Width ratio $\frac{H}{T}$
 - Nose shape, described by the Bluntness Factor [8, p.429]
- Reynolds number R_e
- displacement thickness of the approach boundary layer δ^* [6]
- free stream turbulence level
- surface roughness
- boundary layers, separations and vortices around the junction

Viscous effects dominate the idealized junction. This concerns the interaction of fuselage and wing boundary layers. The adverse-pressure gradient of the fuselage-nose provokes transition of the boundary-layer and the stagnation point in the wing-body corner (see figure 1.2) induces Vortex systems at the leading edge corner, resulting in a half-elliptic horseshoe-vortex system around upper and lower site of the airfoil. This vortex system is unstable with regard to localization, size and circulation and varies between a single or several large primary vortices, additional secondary vortices and a short period of stable airflow when the vortices are stretched downstream around the wing. A detailed description can be found in [8, p.426]. However, these variations occur at high unsteady frequencies and can therefore be averaged as seen in figure 2. The primary horseshoe vortex has the same rotation as the approach boundary layer vorticity seen in figure 1.2. The smaller secondary vortices are of opposite direction to preserve streamline topology. An abstracted and experimental comparison of these effects can be seen in figure 3.1 and 3.2.

2 Flow around a junction

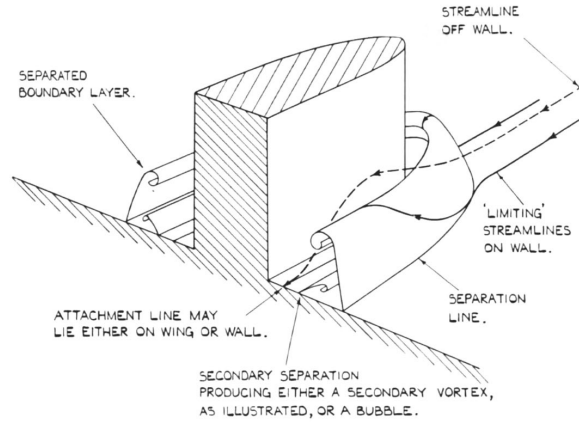
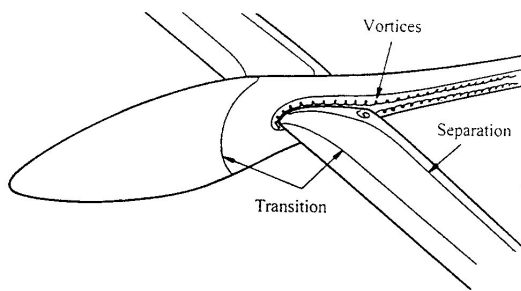
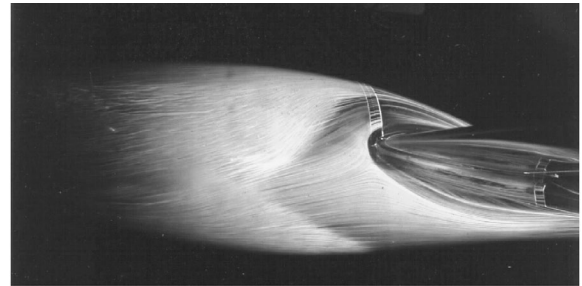


Figure 2: Flow, primary and secondary vortices around the wing root, Reprint from [10]



3.1:



3.2:

Figure 3: 3.1 Viscous flow effects on a high-performance sailplane Reprint from [12]

3.2 Oil flow patterns on the fuselage and wing of a sailplane windtunnel model. view from front to left leading edge Inverted Reprint from [12]

Non-viscous effects regard the streamwise pressure distribution on the wing and body near the junction. In case of a realistic wing-body junction of an aircraft, the influence of a free-shaped fuselage on the airflow is difficult to simulate numerically and was thereby investigated extensively experimental. The first important general effect on streamlines is that, for a positiv (upward) lift coefficient a downward velocity is induced to the flow past the wing chord (see figure4). This causes a reduced angle-of-attack α for the aft fuselage.

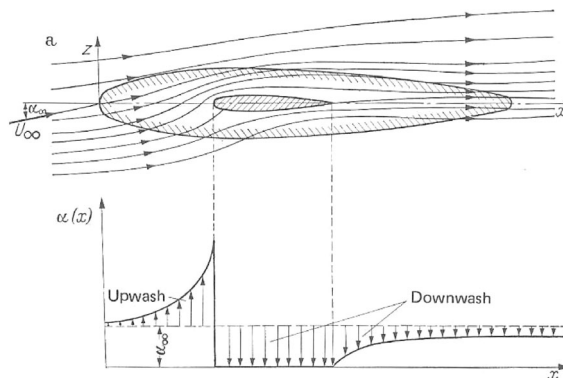


Figure 4: Symmetric streamflow around a wing-body formation and angle-of-attack distribution along the body Reprint from [5, p.306]

Second effect is the so called alpha-flow. With chosen cruising speed and weight, a required lifting coefficient c_l is connected to a certain angle-of-attack α . For lower angles, a downwash around the sides of the fuselage in front of the wing will cause a even more reduced α relative to the wing root. In opposition, for higher angles an upwash and a higher relative α is caused. Because of the higher magnitude of the adverse pressure gradient, the airfoils suction side is stronger influenced by alpha flow (see section 3.1). In figure 3.2 the increased angle-of-attack was visualized.

3 Manipulating the wing-body flow

3.1 wing-body position

The influence on lift and drag of the wing-body relative position was extensively investigated by Jacobs [3, p.584]. In general, results can be summarized in figure 6 and 4. It was shown that:

1. drag coefficient gradient $\frac{\partial c_d}{\partial \alpha}$ increases greatly for wing attachment at top and especially bottom tangent position to the fuselage (See figure 6)
2. short lengthwise position of the wing to the fuselage nose has a small positive effect in reducing parasite drag (see figure 4)

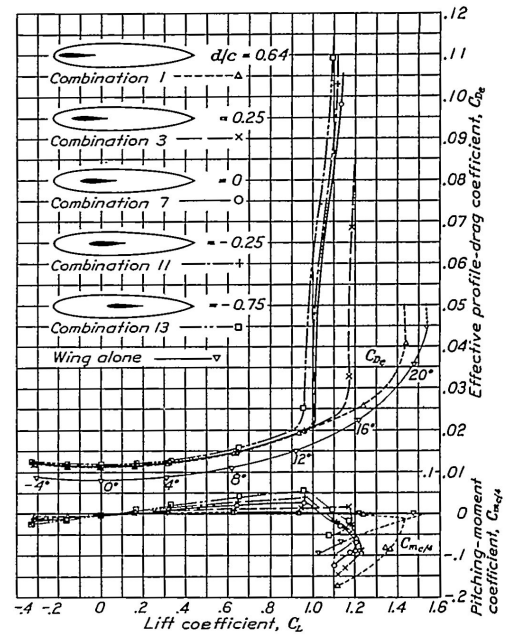


Figure 5: Various fore- and aft-wing positions Reprint from [3]

So the detailed airflow around the airfoil itself differs for low-, mid- or high mounted wings. For this interference the effects can in general be summarized:

- low-mounted wings
 - suction side of the airfoil is heavily influenced by α -flow (see section 2)
 - $\frac{\partial c_d}{\partial \alpha}$ is reduced due to body-caused separation, thereby reduced climbing properties
 - flow separation occurs at a comparatively early chordwise position
 - increased maneuverability because lift attack point is below center of gravity
- mid-mounted wings
 - suction and pressure side of the airfoil are less influenced by the body
 - lift coefficient increase $\frac{\partial c_d}{\partial \alpha}$ is less reduced
 - shortened effective suction spanwidth
 - flow separation occurs at a comparatively average chordwise position
 - well pitchwise balanced, because wing drag attacks near the center of gravity
- high-mounted wings

3 Manipulating the wing-body flow

- the important suction side of the airfoil is only comparative little influenced by the boundary layer of the body
- lift polar is similar, but still more reduced compared to the isolated wing [11, p.170]
- flow separation occurs at a comparatively late chordwise position
- increased stability because lift attack point is higher than center of gravity

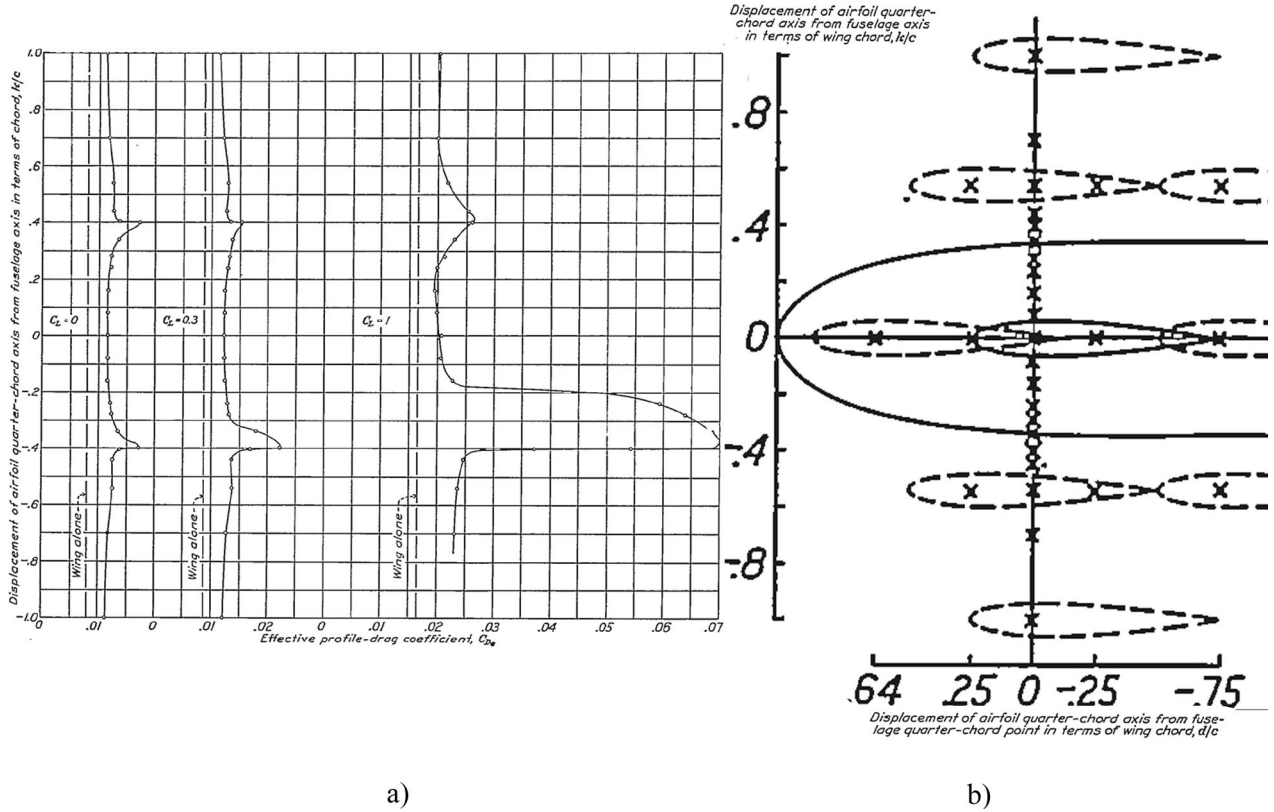


Figure 6: a) Variation of effective drag coefficient with vertical unfilleted and unfaired wing position. Reprint from [3]
 b) Various wing position with respect to fuselage Reprint from [3]

However it was also shown that, in order to achieve a fitting curvature of the intersection lines, fairings, fillets and fuselage design (see 3.2 and 3.3) at these positions provide the chance to reduce drag to acceptable magnitudes similar to middle or far outer wing mount position. Especially sharp angles between body and wing cause early separation, thereby wider join angles reduce drag. An interesting approach for these wider join angles in combination with cambered high-mounted sailplane wings was done by Boermans [12, pp.8]. However no performance data was submitted, the idea was to connect the wing as high as possible (for reducing α -Flow, see Chapter 2 and fig. 7.2) with an maximum angle to the fuselage to avoid narrow junctions. In addition, the airfoil is adapted to balance out the spanwise pressure distribution (see fig. 7.1).

For motor-driven airplanes, it is necessary to notice the big influence of possible airscrew downwash and increased Reynolds Numbers and turbulence of the free stream (see 3.2) around the junction, thereby maybe diminishing all previous efforts.

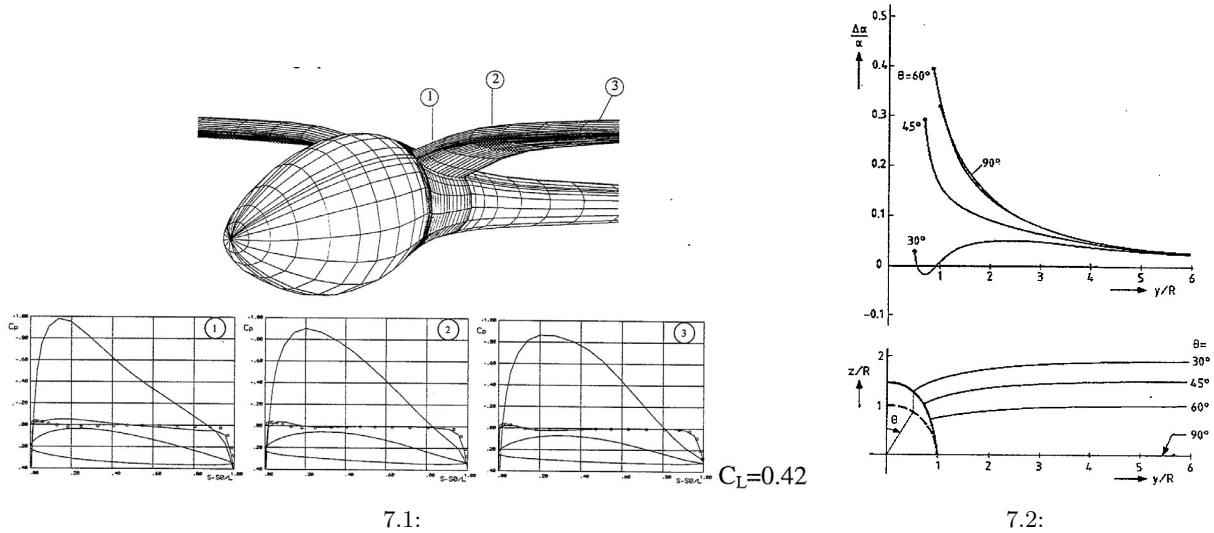


Figure 7: 7.1 Pressure distributions for a sailplane high-mounted wing-fuselage with spanwise cambered wing Reprint from [12]
 7.2 Flow angle at leading edge of wings cambered along equipotential lines Reprint from [12]

3.2 Fillets and Fairings

Fairings White did extensive research[14] on a 1929 low-wing motorplane wing-body junction and measured greatly reduced separation and drag for a faired root wing under higher angles of attack (See figure 8.1 and 8.2. The shape was complex and aimed towards tangent surface smoothing with consideration of chordwise increasing radii between suction side and fuselage. However the fillet substantially reduced drag for power-off (-30% for $c_l = 1$) as seen in figure 3.2, its influence depended little on fillet size (1-2 %) and is reduced for powered-on airscrew (e.g. high turbulent airflow) to 5%. A practice-oriented approach was realized by Truemper [16] on his small low-winged motorplane. The Idea was to compensate a fuselage-induced spanwise airflow and the resulting loss of lift by increasing the local angle-of-attack α at the wing-root through a fairing similar, but much smaller than this from Fig. 8.2. Several benefits were mentioned: 1) Small attitude changes without sudden deterioration of airspeed, 2) decreased sink rate (from $1000 \frac{ft}{min}$ to $650 \frac{ft}{min}$) and 3) $+5Kn$ TAS for low-power speed. These magnitudes were however obtained under non-reliable conditions in free flight.

Leading edge fillets and the shape of their intersection with the fuselage are of even greater importance because of the described vortex phenomena (see section 2). An elementary study was carried out by Maughmer et al. [15]. It investigated drag and chordwise pressure distribution for different leading edge nose shape thickness and parabolic or linear planforms of the intersection.(see figure 9.1). It turned out that a sharp (Integration geometry 3) and linear (planform B) fillet reduced drag up to 3% for an already aerodynamically very clean sailplane. Thicker nose shapes and a parabolic planform did not improve characteristics, rather increased drag (see figure 9.3) and decreased pressure coefficient c_p (see figure 9.4).

3 Manipulating the wing-body flow



8.1:



8.2:

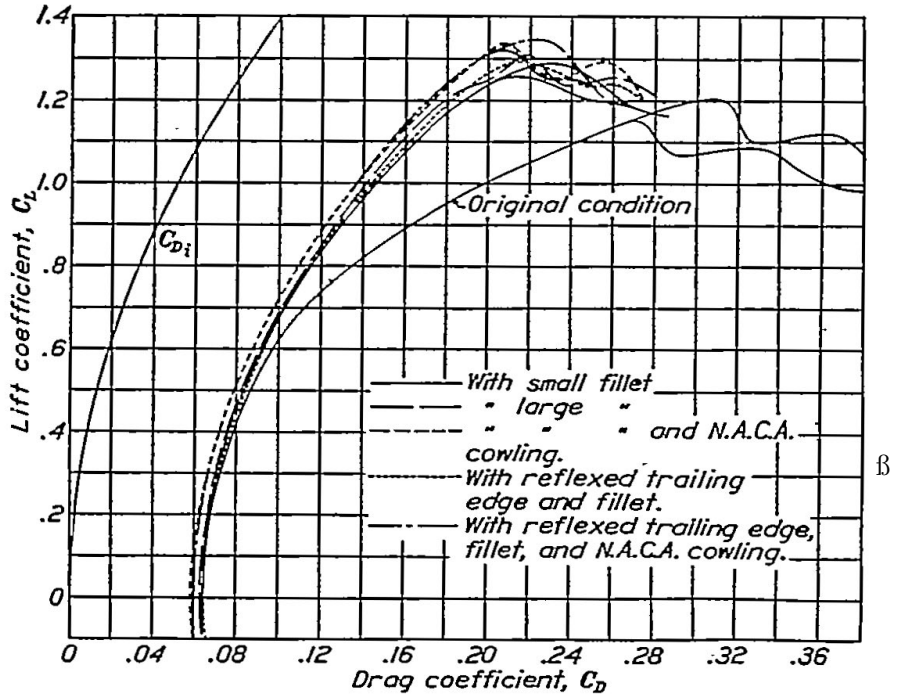
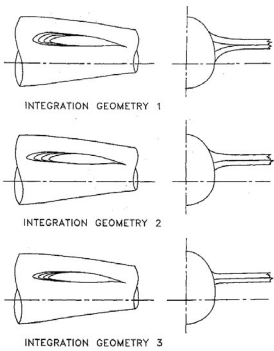


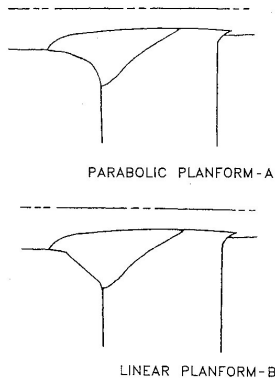
Figure 8: Polars for McDonnell airplane with various fillets. Power off. Reprint from [14]

8.1 Unfaired original wing-fuselage intersection of McDonnell airplane. Reprint from [14]

8.2 Large wing root fairing and fillet on McDonnell airplane Reprint from [14]



9.1:



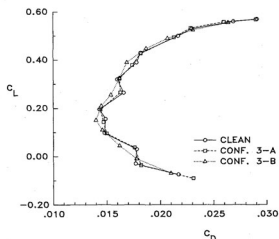
9.2:

Figure 9: 9.1 Profiles and front view of wing-fuselage integration geometries Reprint from [15]

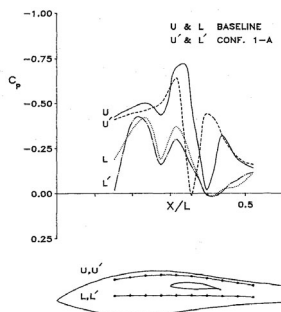
9.2 Planform views of wing-fuselage integration geometries Reprint from [15]

9.3 Drag polar comparison of baseline sailplane to those modified using integration geometry 3 $R_e = 4 \cdot 10^5$ Reprint from [15]

9.4 Comparison of pressure distributions along fuselage lines for baseline and modified configurations, $\alpha = 4.5^\circ$ Reprint from [15]



9.3:



9.4:

Trailing edge fillets and the effect of different shapes for the wing-root junction were investigated earlier by Muttray [2], who suggested backward increasing radii for the wing-body trailing edge fillet of sailplanes, so that in planview the wings joints tangent the fuselage. This showed only very little effect, decreasing c_w -polar around -4% for very high $c_l = 1.4$. White also investigated the effect of a reflexed (spanwise different chordlength) trailing edge, but found the aerodynamic effects negligible (see Chapter 3.2). A recent, more intuitive use of this theory was made by Arnold [22], but his Arnold AR-5 trailing-edge design stands in the tradition of well-performing world-war II fighter-planes (see fig. 10.1-10.3)

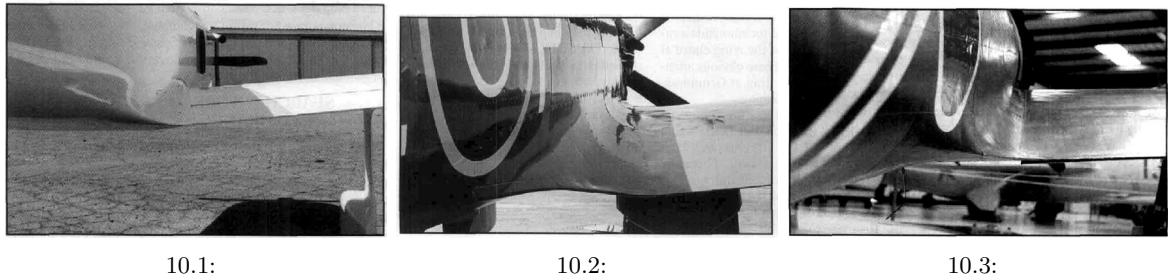


Figure 10: Trailing-edge fillets of different sizes From left:Arnold AR-5, Supermarine Spitfire, Mitsubishi Zero Reprint from [22]

3.3 Fuselage design

Boermans [12, p.3] stated for sailplanes that high performance fuselage design is reached through stream-line fitted body-shaping. So the fuselage is contracted in height and width to achieve a streamlined fuselage shape for a certain, most-occurring flight condition 2, in most cases the lift coefficient c_l for best glide ratio. As it can be seen in figure 11.1, the change of friction at transition and zero friction at separation are clearly visible in the oil flow. Also visible is the line where zig-zag-stripes trip the boundary layer causing small vortices. The width contraction is carefully optimised, with different results up to decreasing drag of the shape c_{d_s} by 40%. For too high contractions (variants 3 and 4 in fig.11.2 the boundary layer can not follow the shape and the steep adverse pressure causes the boundary layer to separate.

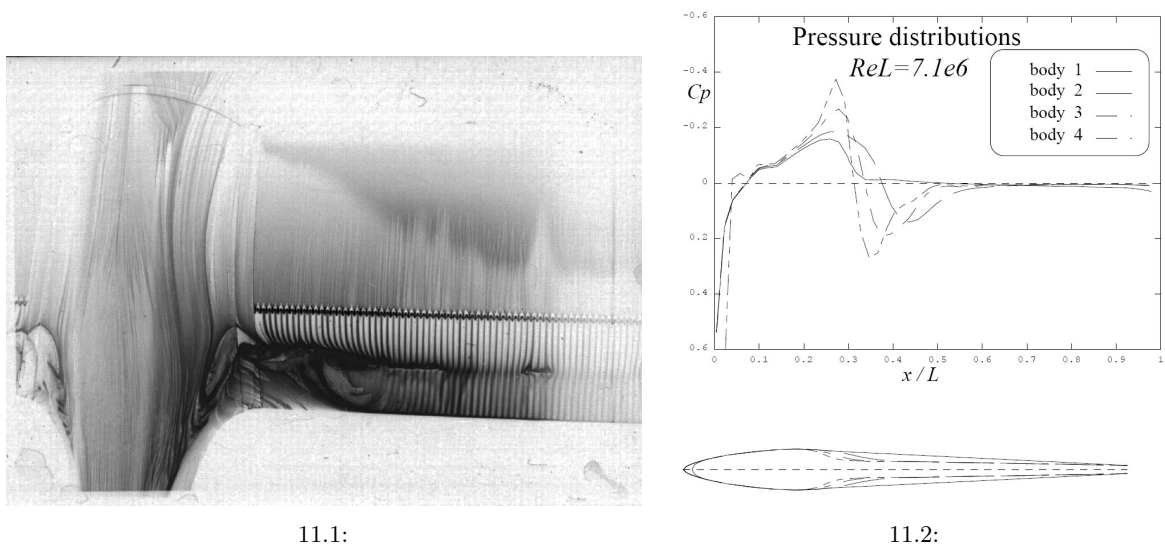


Figure 11: 11.1 Oil flow patterns on the upper side of a high-performance sailplane model in wind-tunnel Reprint from [13]
 11.2 Althaus axisymmetric profiles Reprint from [13]

3 Manipulating the wing-body flow

The turbulent separated area on the trailing edge/wing corner (as seen in fig.11.1 and 12.1) was the interest in an investigation for much bigger aircrafts done by Vassberg et al. [17] concerning numerical drag prediction. The first goal was to prevent this separated area for a near-sonic ($Ma_\infty = 0.75$) flying prototype DLR-F6. To achieve this, a big side-of-body fairing (FX1) was developed, significantly increasing the included-angle between upper wing trailing edge and fuselage (see fig. 12.5). The second goal was to attach the stream completely onto the rearwing/fuselage corner. Following the basic principle, that shape has to follow stream, a second fairing (FX2) was attached (see fig. 12.7). Although the goals were numerically reached, drag decrease and magnitudes for drag were not part of this study. But to clarify the importance of these investigations, an U.S.patent by Airbus should be mentioned here [18], that describes a variable shape along the chordwise junction line to influence the pressure distribution on the wing. The goal was to adjust it to the pressure influence of different engine nacelles.

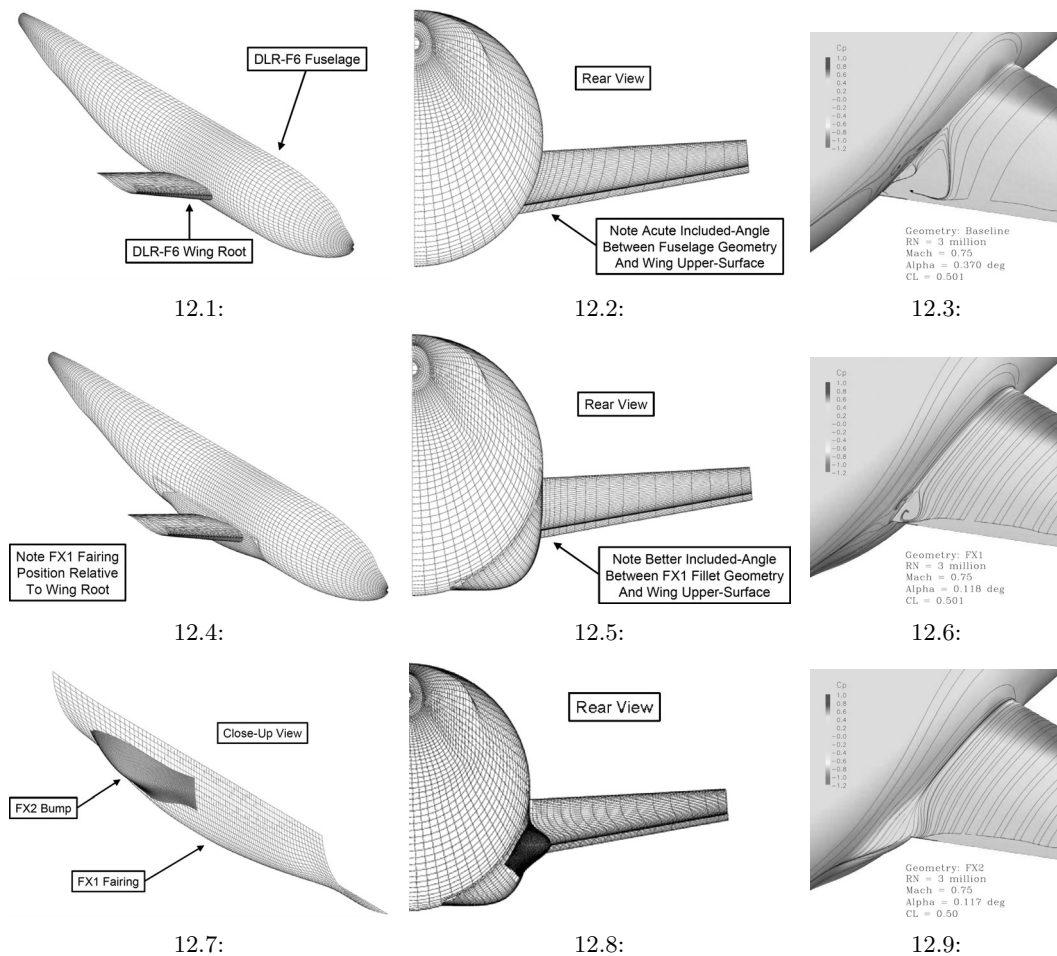


Figure 12: first row : DLR-F6 fuselage with section of wing root
 second row: DLR-F6 fuselage with FX1 fairing
 third row : DLR-F6 fuselage with FX1 fairing and FX2 bump fairing
 Reprint from [17]

Another very intuitive approach for decreasing drag was published by Arnold [22], designer of AR-X motorplanes, known for high performance (topspeed to horsepower ratio). He claimed, that the position of the canopy relative to the wing-body junction is of great importance and the pressure distributions have to be adapted to each other (see fig. 13.) However this theory is not proven, one has to admit that his airplanes are of very small drag area and the wing-fuselage interference has only an influence of 3.8% on the whole drag(see [23]).

3 Manipulating the wing-body flow

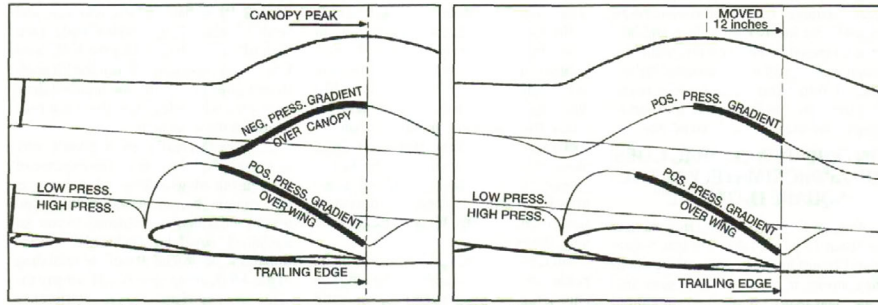


Figure 13: pressure gradients unmatched (left) and matched (right) for Arnolds AR-5 during climbing flight Reprint from [22]

3.4 other approaches

A first approach to eliminate the vorticity and thereby reduce the drag was made by Philipps [19], who removed the approach boundary layer through a rectangle hole in front of a wall-mounted cylinder. However this attempt was mostly succesful, almost double the boundary layer volume had to be sucked in, and still the suction hole itself caused little vortices. A very similar approach was made by Barberis et Al. [20], trying to decrease vorticity either by a small obstacle or a suction hole in front of a wall-mounted Tail-cylinder (Rood-Wing) (see fig. 14.1 and 14.2). Flow visualization is given for average speed of $v_\infty = 50 \frac{m}{s}$. The obstacle had little effect except energizing the boundary layer, but the suction device decreased vorticity reasonably. If the airflow is faster and Reynolds number increase, influence effects diminish. A wider approach on decreasing drag by state-of-the-art technologies was summarized by Jahanniri [21], including the influence viscous drag, drag due to lift and wave drag not only for the wing-body junction.

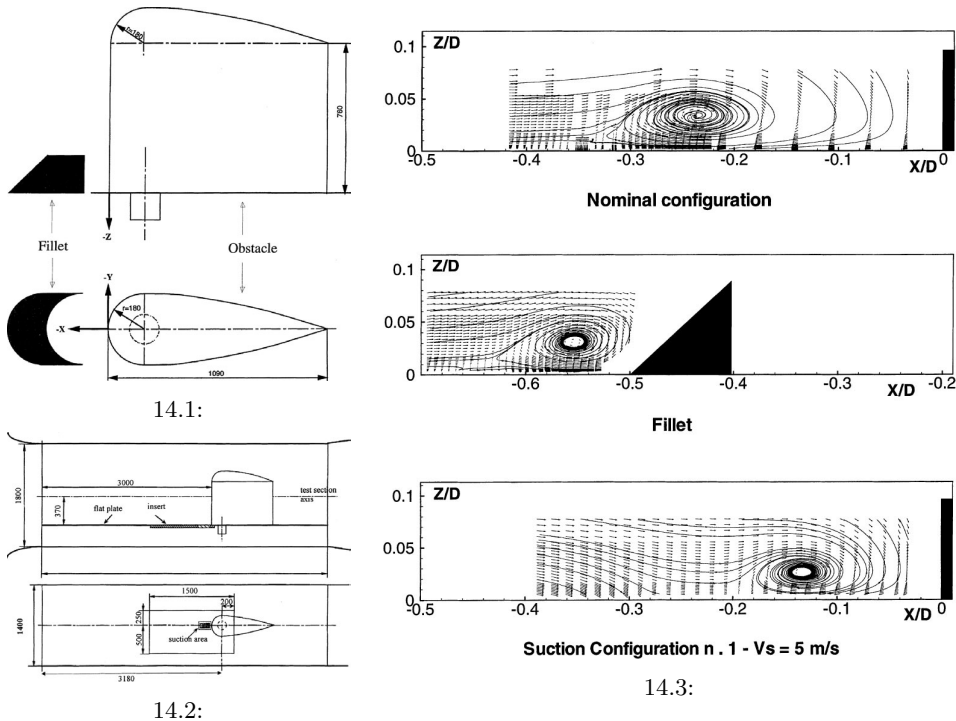


Figure 14: 14.1 Definition of obstacle and fillet All Reprints from [20]

14.2 Experimental arrangement of the suction device

14.3 Mean velocity vector and streamlines: Plane of symmetry $v_\infty = 50 \frac{m}{s}$

References

- [1] Muttray, H., Versuche über die Ausbildung der Flügelwurzel, Ergebnisse der Aerodynamischen Versuchsanstalt Göttingen, Verlag R. Oldenburg 1932, III.8, pp.89
- [2] Muttray, H., Aerodynamic aspects of wing-fuselage fillets, NACA Technical Memorandum No. 764, National Advisory Committee for Aeronautics 1935
- [3] Jacobs, E. and Ward, K., Interference of wing and fuselage from tests of 209 combinations in the NACA variable-density test tunnel, NACA Technical Report No. 540, National Advisory Committee for Aeronautics 1935
- [4] Hoerner, S.F., Fluid Dynamic Drag, Hoerner Fluid Dynamics 1965
- [5] Schlichting, H. and Truckenbrodt, E., Aerodynamics of the Aeroplane, McGraw Hill Higher Education; 2nd edition 1979
- [6] Fleming, J., Simpson, R., Cowling, J. and Devenport, W. An experimental study of a turbulent wing-body junction and wake flow, Experiments in Fluids 14, 1993 p.366-378
- [7] Öelcmen, S, and Simpson, R. Some structural features of a turbulent wing-body junction vortical flow, Report No. VPI-AOE-238, Virginia Polytechnic Institute and State University Blacksburg 1996
- [8] Simpson, R. Junction Flows, Annual Review of Fluid Mechanics; 33, ProQuest Science Journals pg. 415 2001
- [9] Walter, J., Measurements in Three-Dimensional Wake of a Surface-Mounted Winglike Symmetrical Ellipsoid Experimental Thermal and Fluid Science 13:266-291 1996
- [10] Stanbrook, A Experimental Observation of Vortices in Wing-Body Junctions, R.A.E. Report Aero. 2589, Ministry of supply Reports and Memoranda No. 3114 1957
- [11] Althaus, D., Wind Tunnel Measurements on Bodies and Wing-Body Combinations, Motorless Flight Research, NASA Contractor Report 2315 pp.155, 1973
- [12] Boermans, L.M.M., Nicolosi, F and Kubrynski, K. Aerodynamic design of high performance sailplane wing fuselage combinations, presented at the International Council of the Aeronautical Sciences, Paper No.A98-31523 1998
- [13] Boermans, L.M.M., Research on sailplane aerodynamics at Delft University of Technology. Recent and present developments Presentation paper for the Netherlands Association of Aeronautical Engineers (NVvL) on 1 June 2006
- [14] White, James A. and Hood, Manley J., Wing-Fuselage Interference Tail buffeting and air flow about the tail of a low wing monoplane NACA Technical Report No.482, National Advisory Committee for Aeronautics 1933
- [15] Maughmer, M., Hallmann, D., Ruszkowski, R., Chappel, G., Waitz, I., Experimental Investigations of Wing-Fuselage Integration Geometries AIAA paper 87 2937, AIAA Journal of Aircraft Vol.26, No.8, 1989
- [16] Truemper, Klaus, Finding Hidden Drag Hangar Echoes V.31 Issue 4 p.9, Experimental Aircraft Association, Dallas/Texas, 2009
- [17] Vassber, J. Sciafani, A. and DeHaan, M. A Wing-Body Fairing Design for the DLR-F6 Model: A DPW-III Case Study AIAA Conference paper 2005-4730

References

- [18] Fol, Thierry, Jimenez, P. and Arnaud, N. Aircraft compromising a central fairing that adjusts the pressure on the wing structure by means of local geometric deformations US 2009/0078830 A1
- [19] Philipps, D.B., Cembala, J.M. An experimental investigation of the effects of body surface suction on the vortex Technical Report No. Tr 91-016, Pennsylvania State Laboratory, 1990
- [20] D. Barberis, P. Molton, T. Malaterre Control of 3D turbulent boundary layer separation caused by a wing-body junction Experimental Thermal and Fluid Science 16, p.54-63, 1998
- [21] Jahanmiri, M. Aircraft Drag Reduction: An Overview Research report 2011:02, CHALMERS UNIVERSITY OF TECHNOLOGY, 2011
- [22] Arnold, Mike Inverse pressure gradient matching Sport Aviation, p.61-67, May 1997
- [23] Carmichael, Bruce Drag analysis of the Arnold AR-5 airplane CONTACT Magazine, Vol 5, Number 1, Jan - Feb 1994, Issue 24

The author thanks Peter Gasparovic for motivation and academic advise and Jan Pila, Pavol Bajusz and the Department of Engineering for providing organisational support during the IAESTE exchange program.